Numerical studies of acceleration of thorium ions by a laser pulse of ultra-relativistic intensity

Jaroslaw Domanski[*], and *Jan* Badziak

Institute of Plasma Physics and Laser Mirofusion, 01-497 Warsaw, Poland

Abstract. One of the key scientific projects of ELI-Nuclear Physics is to study the production of extremely neutron-rich nuclides by a new reaction mechanism called fission-fusion using laser-accelerated thorium (^{232}Th) ions. This research is of crucial importance for understanding the nature of the creation of heavy elements in the Universe; however, they require Th ion beams of very high beam fluencies and intensities which are inaccessible in conventional accelerators. This contribution is a first attempt to investigate the possibility of the generation of intense Th ion beams by a fs laser pulse of ultra-relativistic intensity. The investigation was performed with the use of fully electromagnetic relativistic particle-in-cell code. A sub-μm thorium target was irradiated by a circularly polarized 20-fs laser pulse of intensity up to 10^{23} W/cm^2, predicted to be attainable at ELI-NP. At the laser intensity $\sim 10^{23}$ W/cm^2 and an optimum target thickness, the maximum energies of Th ions approach 9.3 GeV, the ion beam intensity is $> 10^{20}$ W/cm^2 and the total ion fluence reaches values $\sim 10^{19}$ ions/cm^2. The last two values are much higher than attainable in conventional accelerators and are fairly promising for the planned ELI-NP experiment.

1 Introduction

There are several different ways that heavy elements are produced in the Universe. Elements up to iron are produced via the thermonuclear fusion process in stars. Heavier nuclei could be produced in the slow neutron capture process (s-process) along the valley of stability. This process occurs inside the asymptotic giant branch (AGB) stars and lead to about half of the heavier nuclei [1,2]. The rest of the heavier nuclei are produced via a rapid neutron capture process (r-process). The astrophysical site of the r-process nucleosynthesis is still under debate: it may be cataclysmic core collapse supernovae (II) explosions with neutrino winds [2,3] or mergers of neutron-star binaries [2,4]. While the lower-mass path of the r-process for the production of heavy elements is well explored, the nuclei around the N = 126 (number of neutrons) waiting point critically determine this element production mechanism. At present, basically nothing is known about these nuclei [2]. For this reason an experiment was proposed for ELI-Nuclear Physics (ELI-NP) laser facility in which extremely neutron rich nuclei from this region will be produced via the fission-fusion reaction mechanism.

ELI-NP is a currently build large European research facility that will produce multi-PW femtosecond laser pulses of ultra-relativistic intensity ($\sim 10^{23}$ W/cm^2) to perform research in laser-based nuclear physics and related applications [5]. In the basic concept of the fission-fusion reaction mechanism [2,6], fissile isotopes (like ^{232}Th) accelerated by an intense laser pulse will enable the interaction of a dense beam of fission

fragments with a second target, also consisting of fissile isotopes. So finally in a second step of the reaction process, fusion between (neutron-rich) beam-like and target-like (light) fission products will become possible, generating extremely neutron-rich ion species. A fission-fusion reaction scenario was proposed for the experiment, wherein the accelerated thorium ions will be fissioned in the CH_2 layer of the reaction target. Furthermore, the accelerated carbon ions and deuterons from the production target generate thorium fragments in the thick thorium layer of the reaction target. This scenario is more efficient than the one where fission would be induced by the thorium ions only. The required parameters for Th ion beams in this scenario are: energy $-E_i/A=7$ MeV/nucleon, fluence $- F_i=10^{18}$ ion/cm^2 and number of ions - $N_i=10^{11}$ [2,6].

This paper is a first attempt to investigate the possibility of the generation of intense Th ion beams by a fs laser pulse of ultra-relativistic intensity. The investigation was performed with the use of fully electromagnetic relativistic multi-dimensional (2D3V) particle-in-cell code. The code was elaborated at the Institute of Plasma Physics and Laser Microfusion and verified for example by a comparison of the results obtained using the code with the ones from measurements presented in [7,8] as well as with the results of 3D simulations of carbon ion acceleration carried out by [9]. The numerical simulations were performed for flat or spherical thorium targets of thickness ranging from 25 nm to 700 nm (which corresponds to the areal mass density from 0.07 mg/cm^2 to 0.9 mg/cm^2) and the transverse dimension equal to 12

---

[*] Corresponding author: jaroslaw.domanski@ifpilm.pl

µm. Molecular density of the target corresponded to the solid-state density and was equal to $3.04*10^{22}$ molecules/cm^3 and the ionization level of Th was assumed to 10. A pre-plasma layer of 0.25 µm thickness and the density shape described by an exponential function was placed in front of the target. The target was irradiated by a circularly polarized 20 fs laser pulse of intensity up to 10^{23} W/cm^2 and energy equal to 150 J predicted to be attainable at ELI-NP. The laser beam shape in time and space (along the y-axis) was described by a super-Gaussian function of the power index equal to 6. The laser beam width (FWHM-Full Width at Half Maximum) was ranging from 3µm to 9 µm and the laser wavelength was equal to 800nm.
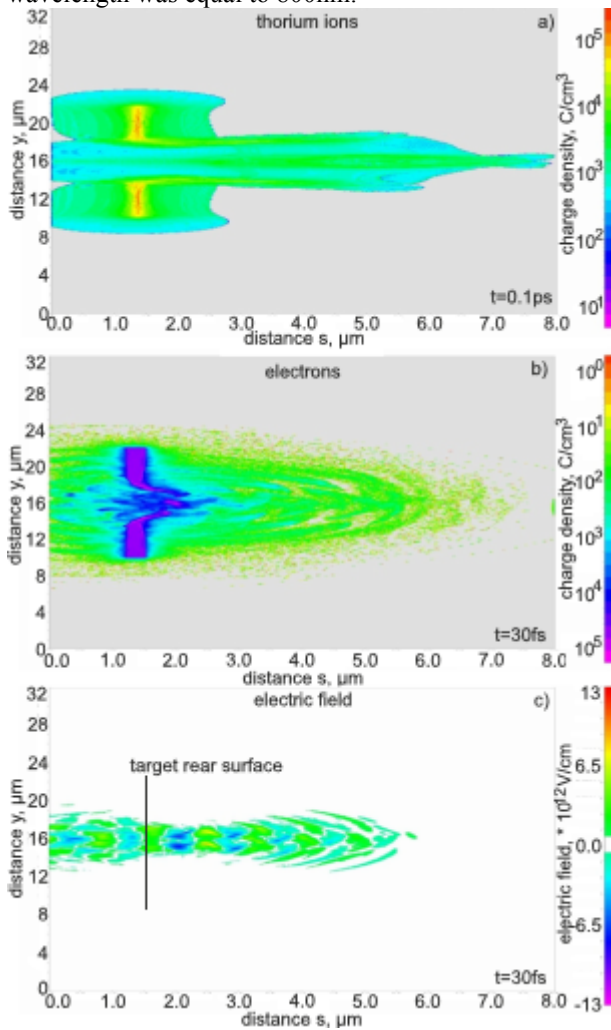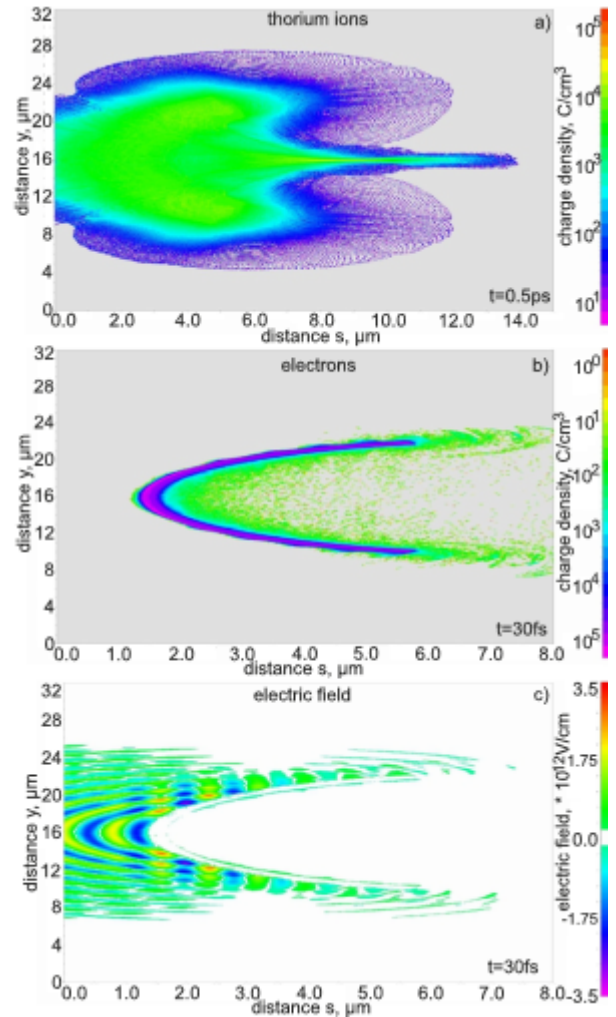

Fig. 1. 2D spatial distribution of charge density of thorium ions (a), electrons (b) and component of electric field parallel to the y axis (c). The 300 nm (0.4mg/cm^2) thick flat target was irradiated by the laser beam of 3µm in diameter and intensity equal to 10^{23} W/cm^2. The simulation time t=0.1ps for (a) and t=30fs for (b,c)

Fig. 2. 2D spatial distribution of charge density of thorium ions (a), electrons (b) and component of electric field parallel to the y axis (c). The 400 nm (0.5mg/cm^2) thick hemispherical target was irradiated by the laser beam of 9µm in diameter and intensity equal to $1.1*10^{22}$W/cm^2. The simulation time t=0.5ps for (a) and t=30fs for (b,c)

2 Results and discussion

Figures 1 and 2 present a 2D spatial distributions of charge density of thorium ions (a), electrons (b) and the component of electric field parallel to the y axis (c). The 300 nm (0.4mg/cm^2) thick flat target (Fig.1) and the 400nm (0.5mg/cm^2) thick hemispherical target (Fig.2) were irradiated by the laser beams of 3 µm (Fig.1) and 9 µm (Fig.2) diameters. The beam intensity was equal to $1.0*10^{23}$ W/cm^2 for the flat target and $1.1*10^{22}$ W/cm^2 for the hemispherical one. For both considered cases the laser pulse parameters correspond to the radiation pressure acceleration (RPA) mechanism domination range [10,11,12,13]. However, for the flat target the relativistic transparency [14,15] of the target is observed (Fig.1c) since the electron density in the interaction area decreases below the relativistic critical density (e* n_{cr-rel}=3.0*10^4 C/cm^3). The relativistic transparency is the main reason here for the broad energy (velocity) spectrum of accelerated ions (Fig.1a). In case of the

---
* Corresponding author: jaroslaw.domanski@ifpilm.pl

hemispherical target, the electron density in the target remain higher than the relativistic critical density (e* n_{cr-rel}=9.8*10^3 C/cm^3) and the target is not transparent for the light (Fig, 2c). However, the target is also penetrated by the laser pulse (the ions are not compressed by the laser pulse as effective as electrons) and the energy spectrum of accelerated ions is also broad.

The maximum ion energies as a function of target thickness (a), target focal length and laser beam diameter (b) is shown in Fig. 3. The results in Fig.3a correspond to the flat targets irradiated by the 3µm laser beam. The thickness of the targets for data in Fig.3b is equal to 400nm. It is visible that relativistic transparency of the targets hinders the achievement of high acceleration efficiency for thin targets (< 300nm) (Fig. 3a). Furthermore, the weak influence of the target shape on
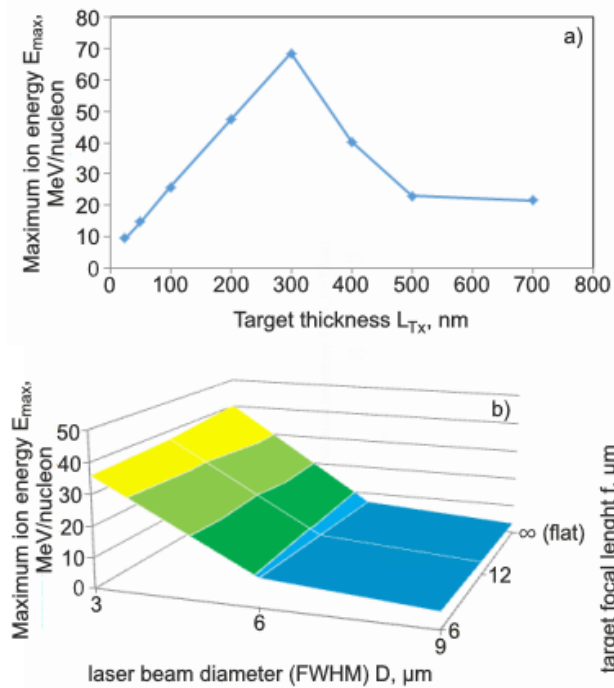

Fig. 3. The maximum ion energy as a function of the flat target thickness (a), and as a function of the hemispherical target focal length and the laser beam diameter (b). For all cases in figure (b) the targets are 400 nm thick. The laser beams energy is equal to 150 J.

the maximum ion energies is observed. Finally, it is worth mentioning that for all investigated cases the ion energy spectra are broad and the standard energy deviations expressed in the mean energy units are higher than one (Fig.4). Despite these unfavorable factors, the maximum thorium ion energies are much higher than required in experiment [2,6] and reach 70 MeV/nucleon.

From the point of view of the proposed nuclear experiment [2,6], the characteristics of ion beam such as the beam intensity, diameter and fluence as well as the total number of accelerated ions are also important. Figure 5 presents the maximum ion beam intensity (a) and the ion beam diameter (b), recorded 10 µm behind the rear surface of the target, as a function of the flat target thickness. For all investigated cases the laser beam

---

*
Corresponding author: jaroslaw.domanski@ifpilm.pl

diameter on the target is equal to 3 µm. The intensity of ion beam is higher for thicker targets (≥300nm) and the best results is achieved for the 400nm, the thinnest
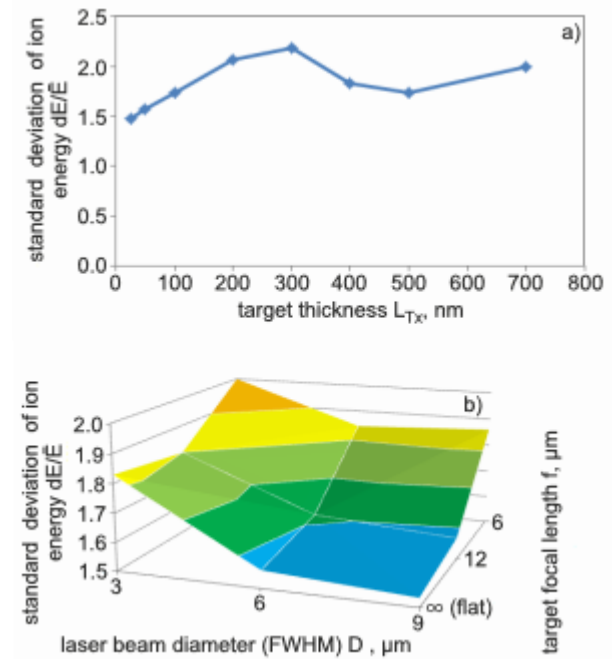

Fig. 4. The standard deviation of ion energy as a function of the flat target thickness (a), and as a function of the hemispherical target focal length and the laser beam diameter (b). For all cases in figure (b) the targets are 400nm thick. The laser beams energy is equal to 150 J.
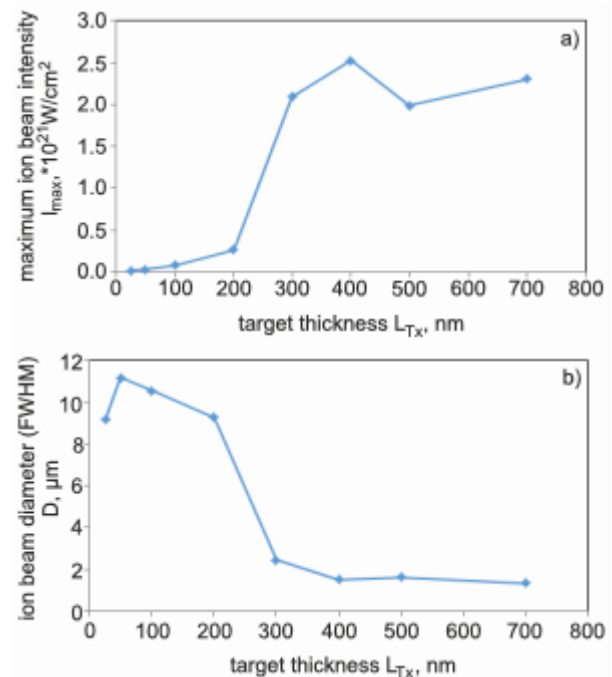

Fig. 5. The maximum ion beam intensity (a) and the ion beam diameter (b), recorded 10 µm behind the target rear surface, as a function of the flat target thickness. For all investigated cases the laser beam diameter is equal to 3 µm.

opaque, target. In this case the ion beam of intensity of 2.5*10^{21} W/cm^2 and diameter of 1.5 µm is produced.

The maximum ion beam intensity (a) and the ion beam diameter (b) as a function of the hemispherical target focal length and the laser beam diameter is shown

in figure 6. The target thickness is fixed at 400 nm, the value which ensures the highest ion beam intensity for the flat targets. For the 3 μm laser beam and the target of the focal length equal to 6 μm the ion beam of the highest intensity is produced. In this case the intensity is equal to $8*10^{21}$ W/cm^2, the beam width is ~1μm, the maximum thorium ion energy is ~9,3 GeV (40MeV/nucleon) and the ion pulse duration is ~70 fs.
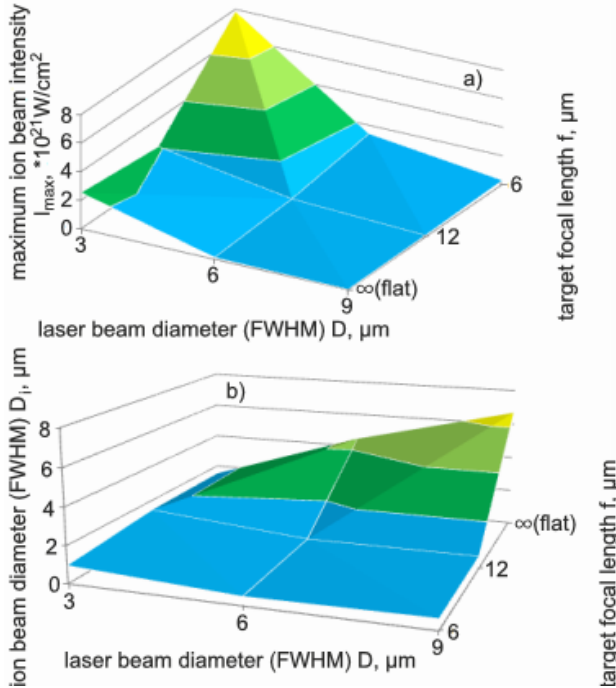

Fig. 6. The maximum ion beam intensity (a) and ion beam diameter (b) as a function of target focal length and laser beam diameter. The target thickness is fixed on 400 nm.

The estimated ion fluence is equal to $7.0*10^{18}$ ion/cm^2 and is even higher than required in the experiment. Furthermore, it is worth mentioning that curving the target leads to focusing of the ion beam and increasing of the beam intensity which is clearly visible in figure 6 and also in figure 2a.

The electron distribution in plasma does not cover exactly the thorium ion distribution and locally the net electric charge in the plasma is different from zero. The inhomogeneous distribution of the charge in the plasma leads to the generation of electric current with the total net value $J=J_{Th}-J_e$ of which can be fairly high (J_e and J_{Th} are the electron current and the thorium ion current, respectively). The total current J changes in time and is inhomogeneously distributed in space as demonstrated in figures 7 and 8. Fig. 7 presents the temporal run of the total current (integrated over the whole transverse size of the simulation box) at the distance of 10 μm from the target rear surface while Fig.8 shows the transverse distribution of the current density at this distance at t=325fs. The comparison of the results for flat 400 nm thick and hemispherical (D$_i$=6μm) targets irradiated by laser pulse of intensity equal to 10^{23} W/cm^2 and 3μm diameter is presented. It can be seen that the structure of the total current distribution is similar for both types of investigated targets and is also similar to that obtained for CH target [16]. It is also visible that at the time

*Corresponding author: jaroslaw.domanski@ifpilm.pl

longer than 200fs (an order of magnitude longer than the laser pulse) the total current is dominated by fast electrons (the current is negative) and reaches the value of several MA both for flat and hemispherical targets. However, the maximum value of the current is clearly higher for the hemispherical target. This strong flux of
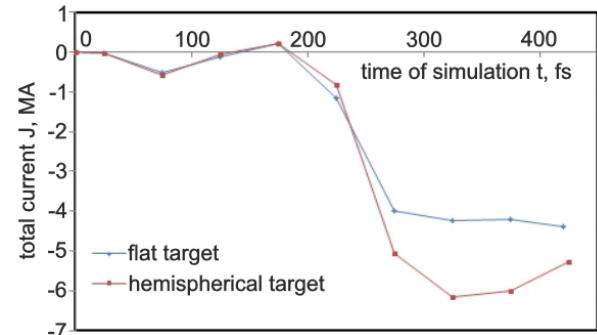

Fig. 7. The temporal run of the total current in the thorium plasma (integrated over the whole transverse size of the simulation box) at the distance of 10 μm from the rear surface of the target. The comparison of the results for the 400-nm flat and hemispherical (D$_i$=6μm) targets irradiated by the laser beam of intensity of 10^{23} W/cm^2 and diameter of 3μm.

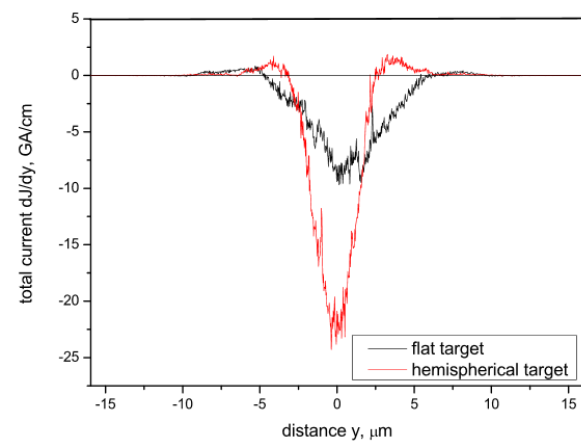**Fig. 8.** The transverse distribution of the current density at the distance of 10 μm from the rear surface of the target at t=325fs. The comparison of the results for the 400-nm flat and hemispherical (D$_i$=6μm) targets irradiated by the laser beam of intensity of 10^{23} W/cm^2 and diameter of 3μm.

fast electron escaping from the target is the generator of an intense electromagnetic emission (usually in THz domain of frequency) and moreover, it is the cause of the creation of net positive charge of the target (an electric neutrality of the target is disturbed by loss of negative charge carried by the fast electron flux). The neutralization current flowing through the target and the target holder can be the source of a strong electromagnetic pulse (EMP), usually in the (0.1 – 10) GHz domain which propagates into the interaction chamber and may be very detrimental for diagnostic equipment and other electronic devices [17,18]. The strength of EMP is proportional to the power of the laser pulse interacting with the target. For this reason the problem of EMP generated in the laser-target interaction is currently a hot topic intensely studied and is especially important for multi-PW laser facilities like ELI. The results presented in this paper show briefly the way the

fundamental source of EMP is created in the initial stage of the process when the ion beam is formed and accelerated due to the laser-target interaction. More detailed analysis of this issue will be presented in our other paper.

3 Conclusions

In conclusion, the generation of intense Th ion beams by a fs laser pulse of ultra-relativistic intensity has been investigated with the use of relativistic 2D3V particle-in-cell code. A sub-µm thorium target was irradiated by a circularly polarized 20-fs laser pulse of intensity up to 10^{23} W/cm^2 predicted to be attainable at ELI-NP. It was found that a key effect that hinders the achievement of high efficiency of ion acceleration in the considered cases and leads to the broad energy spectrum of accelerated ions is relativistic transparency of the target plasma. Despite this, for the 3 µm laser beam of intensity of 10^{23} W/cm^2 and the hemispherical target of the focal length of 6 µm a thorium ion beam of the maximum ion energy ~9,3 GeV (40MeV/nucleon), the peak beam intensity of $8*10^{21}$ W/cm^2 and the beam fluence of $7.0*10^{18}$ ion/cm^2 is produced. Such ion beam parameters are much higher than attainable in conventional accelerators and are fairly promising for the planned ELI-NP experiment. The key problem which needs to be solved is the broad energy spectrum of the accelerated ions that will be the subject of our further studies.

References

1. R. Gallino, C. Arlandini, M. Busso, M. Lugaro, C. Travaglio, O. Straniero, A. Chieffi, M. Limongi, The Astrophysical Journal **497**,388-403 (1998)

2. F. Negoita, M. Roth, P. G. Thirolf, S. Tudisco, F. Hannachi, S. Moustaizis, I. Pomerantz, P. McKenna, J. Fuchs, K. Sphor, G. Acbas, A. Anzalone, P. Audebert, S. Balascuta, F. Cappuzzello, M. O. Cernaianu, S. Chen, I. Dancus, R. Freeman, H. Geissel, P. Ghenuche, L. Gizzi, F. Gobet, G. Gosselin, M. Gugiu, D. Higginson, E. D'Humieres, C. Ivan, D. Jaroszynski, S. Kar, L. Lamia, V. Leca, L. Neagu, G. Lanzalone, V. Meot, S. R. Mirfayzi, I. O. Mitu, P. Morel, C. Murphy, C. Petcu, H. Petrascu, C. Petrone, P. Raczka, M.Risca, F. Rotaru, J. J. Santos, D. Schumacher, D. Stutman, M. Tarisien, M. Tataru, B. Tatulea, I. C. E. Turcu, M. Versteegen, D. Ursescu, S. Gales, N. V. Zamfir, Romanian Reports in Physics **68**, Supplement, S37-S144 (2016)

3. I. V. Panov, H.-Th. Janka, Astr. Astroph., **494**, 829 (2009)

4. R. Surman, G.C. McLaudhlin, M. Ruffert, H.-Th. Janka, W. R. Hix, The Astrophysical Journal **679**, L117-L120 (2008)

5. C. Danson, D. Hillier, N. Hopps, D. Neely, High Power Sci. Engineering **3**, e3 (2015)

6. D. Habs, P. G. Thirolf, M. Gross, K. Allinger, J. Bin, A. Henig, D. Kiefer, W. Ma, J. Schreiber, Appl. Phys. B **103**, 471 (2011)

7. J. Badziak, S. Jabłoński, P. Parys, M. Rosiński, J. Wołowski, A. Szydłowski, P. Antici, J. Fuchs, A. Mancic, J. Appl. Phys. **104**, 063310 (2008)

8. J. Badziak, P. Antici, J. Fuchs, S. Jabłoński, A. Mancic, P. Parys, M. Rosiński, R. Suchańska, A. Szydłowski, J. Wołowski, AIP Conf. Proc. **1024**, 63-77 (2008)

9. A. Sgattoni, S. Sinigardi, A. Macchi, Appl. Phys. Lett. **105**, 084105 (2014)

10. T. Esirkepov, M. Borghesi, S.V. Bulanov, G. Mourou, T. Tajima, Phys. Rev. Lett. **92**, 175003 (2004)

11. A. P. L. Robinson, M. Zepf, S. Kar, R. G. Evans, C. Bellei, New J. Phys. **10**, 012021 (2008)

12. O. Klimo, J. Piskal, J. Limpouch, V.T. Tikhonchuk, Phys. Rev. ST-Accelerators and Beams **11**, 031301 (2008)

13. T. Schlegel, N. Naumova, V.T. Tikhonchuk, C. Labaune, I. V. Sokolov, G. Mourou, Phys. Plasmas **16**, 083103 (2009)

14. A. Macchi, M. Borghesi, M. Passoni, Rev. Mod. Phys. **85**, 751 (2013)

15. J. Domanski, J. Badziak, S. Jabłonski, Laser Part. Beams **35**, 286-293 (2017)

16. J. Domanski, J. Badziak, S. Jabłonski, Proc. of SPIE **10445**, 1044543-1 (2017)

17. J.-L. Dubois, F. Lubrano-Lavaderci, D. Raffestin, J. Ribolzi, J. Gazave, A. Compant La Fontaine, E. d'Humieres, S. Hulin, Ph. Nicolai, A. Poye, V.T. Tikhonchuk, Phys. Rev. E **89**, 013102 (2014)

18. A. Poye, J.-L. Dubois, F. Lubrano-Lavaderci, E. d'Humieres, M. Bardon, S. Hulin, M. Bailly-Grandvaux, J. Ribolzi, D. Raffestin, J.J. Santos, Ph. Nicolai, V.T. Tikhonchuk, Phys. Rev. E **92**, 043107 (2015)

---

* Corresponding author: jaroslaw.domanski@ifpilm.pl